

LA-UR- 09-00238

Approved for public release;
distribution is unlimited.

Title: Model of Transcriptional Activation by MarA in Escherichia coli

Author(s): Michael E. Wall, CCS-3, Z# 165951
Judah L. Rosner, National Institute of Health
Robert G. Martin, National Institute of Health

Intended for: Submission to Proceedings of the National Academy of Sciences.



Los Alamos National Laboratory, an affirmative action/equal opportunity employer, is operated by the Los Alamos National Security, LLC for the National Nuclear Security Administration of the U.S. Department of Energy under contract DE-AC52-06NA25396. By acceptance of this article, the publisher recognizes that the U.S. Government retains a nonexclusive, royalty-free license to publish or reproduce the published form of this contribution, or to allow others to do so, for U.S. Government purposes. Los Alamos National Laboratory requests that the publisher identify this article as work performed under the auspices of the U.S. Department of Energy. Los Alamos National Laboratory strongly supports academic freedom and a researcher's right to publish; as an institution, however, the Laboratory does not endorse the viewpoint of a publication or guarantee its technical correctness.

Model of Transcriptional Activation by MarA in *Escherichia coli*

Michael E. Wall¹, Judah L. Rosner², Robert G. Martin²

¹ Computer, Computational, and Statistical Sciences Division, Bioscience Division, and Center for Nonlinear Studies, Los Alamos National Laboratory, Los Alamos, NM, USA

² Laboratory of Molecular Biology, National Institute of Diabetes, Digestive and Kidney Diseases, National Institutes of Health, Bethesda, MD, USA

Abstract

We have developed a mathematical model of transcriptional activation by MarA in *Escherichia coli*, and used the model to analyze measurements of MarA-dependent activity of the *marRAB*, *sodA*, and *micF* promoters in *mar-rob-* cells. The model helps to rationalize an unexpected poor correlation between the mid-point of *in vivo* promoter activity profiles and *in vitro* equilibrium constants for MarA binding to promoter sequences. Analysis of the promoter activity data using the model yielded the following predictions regarding activation mechanisms: (1) MarA activation of the *marRAB*, *sodA*, and *micF* promoters involves a net acceleration of the kinetics of transitions after RNA polymerase binding, up to and including promoter escape and message elongation; (2) RNA polymerase binds to these promoters with nearly unit occupancy in the absence of MarA, making recruitment of polymerase an insignificant factor in activation of these promoters; and (3) instead of recruitment, activation of the *micF* promoter might involve a *repulsion* of polymerase combined with a large acceleration of the kinetics of polymerase activity. Our models of activation of *sodA* and *micF* represent exceptions to the textbook description of activation of bacterial σ^{70} promoters. However, the *sodA* model is consistent with a published assay of interactions between polymerase and the *E. coli* chromosome; in addition, use of accelerated polymerase kinetics instead of recruitment might confer a competitive advantage to *E. coli* by decreasing latency in gene regulation.

Introduction

In the textbook model of transcriptional activation, activator recruits RNA polymerase to the promoter (1-3). Recruitment works purely by increasing the likelihood that there is an enzyme present, poised to synthesize mRNA; it does not require changes in the downstream events that lead to transcription. This scenario currently dominates interpretation of bacterial transcriptional activation data, and has been adopted in statistical-thermodynamic models of transcriptional activation that capture the activator-dependent expression of several promoters in *Escherichia coli* (4, 5).

The simplicity and generality of the recruitment model are appealing; however, mechanisms of transcriptional activation can vary depending on the activator (3), and are sometimes surprising. For example, MerR binds between the -10 and -35 RNA polymerase recognition sequences (6), and might be expected to repress transcription by blocking polymerase interactions with the promoter. Instead of blocking polymerase, however, MerR and related transcription factors such as SoxR (7) activate transcription by extending the DNA between the hexamers to a length more appropriate for open complex formation.

In addition to diversity among activators, a single activator can work differently at different promoters. For example, CRP binds at different locations upstream of the *gal* (-41.5), *lac* (-61.5), and *maltT* (-70.5) promoters in *E. coli*, with diverse consequences for activation (8). Interactions between CRP and polymerase vary for *gal* or *lac*, and activation at *maltT* can involve an accelerated escape of polymerase from the initiation complex, without detectable changes in the events leading up to open complex formation (8, 9).

Like CRP, MarA activates transcription from diverse locations upstream of promoters; in

addition, it binds to an asymmetric recognition motif with opposite orientations depending on the location (10, 11). However, unlike CRP, which is controlled by intracellular cAMP, MarA has only one domain that interacts with both DNA and polymerase, and has no known effectors. In addition, whereas most well-characterized transcription factors, like CRP, are known to function as a dimer or a higher order complex, MarA is a functional monomer.

Because the position and orientation of its recognition motifs are diverse, and its interactions are relatively simple, MarA is an ideal system for studying how activators differentially activate transcription from promoters. In addition, like CRP, MarA is a global regulator: it activates ~40 genes (the *mar/sox/rob* regulon) of the *E. coli* chromosome resulting in different levels of resistance to a wide array of antibiotics and superoxides (see (12) for references). Diversity in transcriptional activation by MarA therefore presumably has important functional consequences for *E. coli*.

To characterize diversity in MarA regulation of promoter activity, we placed the expression of MarA under the control of the LacI repressor, determined the relationship between IPTG concentration and the intracellular concentration of MarA, and examined the expression of 10 promoters of the regulon as a function of activator concentration (13). We found that: (i) the MarA concentrations needed for half-maximal stimulation varied by at least 19-fold among the promoters indicating substantial variation in promoter activities; (ii) only *marRAB*, *micF*, and *sodA* were saturated at the highest level of MarA obtained; and (iii) the correlation between the MarA concentration needed for half-maximal promoter activity *in vivo* and *marbox* binding affinity *in vitro* was poor.

To further characterize the diversity in MarA activation of promoters, we develop here a quantitative model of MarA transcriptional activation of *marRAB*, *micF*, and *sodA*—the only promoters that exhibited saturation at the highest levels of MarA (13). Our model uses a statistical-thermodynamic treatment of promoter states (14), and considers the interaction between activator and polymerase away from the promoter, which, to our knowledge, has not been considered in previous gene regulation models. The model rationalizes the poor correlation between *in vivo* promoter activity profiles and *in vitro* activator binding affinities. It also suggests that there are diverse mechanisms of MarA activation for the *marRAB*, *micF*, and *sodA* promoters.

Model

We considered a statistical-thermodynamic model of promoter states that was originally developed to study transcriptional repression by λ phage repressor (14). The model is illustrated in Fig. 1. In State 0, the promoter is free. This is the reference state with energy $\Delta G_0 = 0$. In State A, MarA is bound at the operator sequence O_A , yielding free energy ΔG_A ; in State R, polymerase is bound at the promoter P , yielding free energy ΔG_R ; and in State X, both MarA and polymerase are bound, yielding free energy ΔG_X . These free energies are defined for 1 M concentrations of “free” MarA (ΔG_A), polymerase (ΔG_R), and MarA-polymerase complex (ΔG_X). (We use a liberal definition of free molecules in which they may be located anywhere away from the promoter, including nonspecific sites on DNA, and use a single effective free energy to characterize the equilibrium with the bound state.)

The free energies of the states are related to corresponding dissociation constants via $\Delta G_i = k_B T \ln K_i$, where K_i is the dissociation constant of state i in molar units. These dissociation constants in turn determine the statistical weights p_i via the following equations:

$$\begin{aligned}
p_A &= \frac{[A]}{K_A} p_0, \\
p_R &= \frac{[R]}{K_R} p_0, \\
p_X &= \frac{[X]}{K_X} p_0, \text{ and} \\
p_0 &= \frac{1}{1 + [A]/K_A + [R]/K_R + [X]/K_X}.
\end{aligned} \tag{1}$$

In Eqs. (1), the first three equations follow from the definition of the dissociation constants, and the last equation follows from the normalization condition $\sum_i p_i = 1$. Consistent with the definitions of free energies in the previous paragraph, the ratios p_i/p_0 for 1 M concentrations of the DNA-binding partner are equal to the Boltzmann factor $e^{-\Delta G_i/k_B T}$.

The equilibrium between free MarA (A) and polymerase (R) and the MarA-polymerase complex (X) is modeled assuming steady-state equilibration characterized by dissociation constant K_{AR} . We assume that interactions with the promoter do not significantly influence the equilibrium. This is a reasonable assumption given an upper limit of 5 relevant promoters per cell, which is the case for the chromosomal reporters used in Ref. (13). The model leads to the following equations

$$\begin{aligned}
K_{AR} &= [A][R]/[X], \\
[R]_T &= [R] + [X], \text{ and} \\
[A]_T &= [A] + [X],
\end{aligned} \tag{2}$$

where $[R]_T$ and $[A]_T$ are the total levels of polymerase and MarA in the cell, respectively. The solution of Eqs. (2) is

$$\begin{aligned}
[A] &= \frac{1}{2} \left[\sqrt{(K_{AR} - [A]_T + [R]_T)^2 + 4[A]_T K_{AR}} - (K_{AR} - [A]_T + [R]_T) \right], \\
[R] &= \frac{1}{2} \left[\sqrt{(K_{AR} + [A]_T - [R]_T)^2 + 4[R]_T K_{AR}} - (K_{AR} + [A]_T - [R]_T) \right], \text{ and} \\
[X] &= [A][R]/K_{AR}.
\end{aligned} \tag{3}$$

For given values of $[R]_T$ and $[A]_T$, Eqs. (4) yield the concentrations that determine the state weights in Eqs. (1).

The total promoter activity is a weighted sum of the activities in each state. No transcription occurs in states 0 or A, in which polymerase is absent from the promoter. Transcription occurs in state R with activity a_R , and in state X with activity a_X ; polymerase is present at the promoter in both of these states. The equation for the total activity a is

$$a = a_R p_R + a_X p_X. \quad (4)$$

We use Eq. (2) to directly model the experimental assays of β -galactosidase activity (13); in doing this, we assume that the underlying promoter activity is proportional to the measured β -galactosidase activity resulting from *lacZ* reporter expression.

Parameter Values

We used a wide range of parameter values to model the MarA-dependent activity of the *marRAB*, *micF*, and *sodA* promoters. In presenting our results, we focus on the values listed in Table I, and later discuss the sensitivity of these results to variations in parameter values. The values in the table and broader ranges were obtained as follows:

K_{AR} . Martin *et al.* (15) measured a 0.3 μM dissociation constant for MarA-polymerase complex formation in a crystallization buffer. We analyzed the model using this value; however, we found that improved fits were obtained using a value of 1.0 μM for K_{AR} . In addition, we are uncertain about the correct value to use *in vivo*, especially considering that we are lumping into K_{AR} the effect of nonspecific interactions of polymerase and MarA with DNA. To account for this uncertainty, and considering that the fit was improved for higher values of K_{AR} , we illustrate the fit using a value of 100 μM ; we also explored values of 0.3 μM and 10 μM . We expect the value

of K_{AR} to be promoter-independent, and therefore only compare models across promoters using the same value of K_{AR} .

K_A . The nominal value of 75 nM for the MarA-*mar* promoter dissociation constant was obtained from the gel retardation assay in Martin *et al.* (15). The nominal value of 2,000 nM for *sodA* was chosen to be consistent with the lack of binding observed in Martin *et al.* (15). The nominal value of 50 nM for *micF* was chosen from a range of measured values from 8 nM to 80 nM, depending on the preparation (R.G. Martin, unpublished results). To determine whether the qualitative conclusions about activation mechanisms are sensitive to the particular value of K_A , we analyzed the model using a wide range of values, 0.25-2,500 nM.

K_R . The value of the effective dissociation constant for polymerase binding to the promoter is unknown and can vary depending on the promoter. Marr & Roberts (16) measured a dissociation constant of 3 nM for the σ^{70} holoenzyme binding to a 19 bp oligonucleotide containing the TATAAT consensus sequence. We analyze models with a range of values from 1 nM (strong binding) to 1,000 nM (weak binding).

K_X . The value of the dissociation constant for the MarA-polymerase complex binding to the promoter is unknown and can vary depending on the promoter. We found reasonable fits by analyzing models in which K_X can be anywhere from 100X smaller to 100X larger than the value of K_R .

$[R]_T$. Ishihama (17) and Mueller-Hill (18) estimate the total number of polymerase molecules in the *E. coli* cell at 2,000 and 3,000, respectively. Although *marRAB*, *micF*, and *sodA* are σ^{70}

promoters, polymerase is distributed among holoenzymes that contain different σ factors in *E. coli*. We used a nominal value of 3,000 copies per cell, and analyzed the sensitivity of the fits to smaller values of 1,000 and 300 copies per cell.

a_R and a_X . For a given set of the above parameter values, these parameters are obtained for a given promoter using Eq. (2) by calculating p_R and p_X for values of $[A]_T$ at which measurements are available, and performing a linear regression.

Results

Calibration of IPTG against MarA. We calibrated IPTG levels against MarA levels using analysis of Western blots in multiple lanes from a single gel (13). The MarA vs. IPTG data are well-described using the equation

$$[A]_T = [A]_{\max} \frac{[I]^h}{[I]^h + K_I^h}, \quad (5)$$

where $[I]$ is the extracellular IPTG concentration, $[A]_T$ is the total cellular MarA concentration that appears in Eqs. (3), $[A]_{\max} = 20,983$ molecules cell⁻¹, $K = 20.132$ mM, and $h = 2.576$ (Supplementary Fig. S1). A measurement at 2 μ M IPTG was discarded because all other data points yielded a best fit that is consistent with zero MarA in the absence of IPTG; this condition was required to explain the sensitivity of promoter activity to low levels of IPTG.

The model is consistent with promoter activation data. For each model of each promoter, we randomly sampled 10,000 sets of parameter values from the nominal ranges in Table I and calculated simulated IPTG-dependent activation profiles. Parameter ranges were sampled in a log uniform manner. Fits were evaluated using a standard χ^2 statistic. The best-fit activation profiles for each promoter are illustrated in Fig. 2; the quality of the fits indicates that the model

is consistent with the observed IPTG-dependent activation of the *marRAB*, *sodA*, and *micF* promoters.

MarA increases polymerase activity. To determine whether polymerase activity changes when MarA is bound to the promoter, we calculated the ratio a_X/a_R for all models. For each model with each set of parameter values, both of these parameters were obtained using Eq. (2) to perform a linear regression (Parameter values). Results are expressed in terms of the acceleration energy, e_a , defined as

$$e_a = -k_B T \ln \frac{a_X}{a_R}. \quad (6)$$

The acceleration energy is equivalent to the activator-induced change in activation energy of a lumped transcription initiation process, under the assumption that a_X and a_R each follow an Arrhenius law with the same attack frequency. A value $e_a = 0$ corresponds to $a_X = a_R$; this condition is consistent with a strict recruitment model of transcriptional activation, in which activator increases the occupancy of polymerase at the promoter but does not alter the kinetics of polymerase activity (1, 3). Models with $e_a < 0$ exhibit acceleration and models with $e_a > 0$ exhibit retardation of polymerase activity in the presence of activator.

The acceleration energy is negative for all 10,000 sets of parameter values in each promoter activation model (Fig. 3, left panels). Activator therefore increases polymerase activity in all promoter activation models. For each promoter, the value of e_a corresponding to the minimum in χ^2 is roughly equal to $k_B T$ (Table II). For all models, χ^2 values sharply increase in the neighborhood of the minimum (Fig. 3), leading to small errors in estimation of the value of e_a (Table II).

Recruitment is not a significant factor in MarA activation of the marRAB and soda promoters. To determine whether the affinity of polymerase for the promoter changes in the presence or absence of MarA, we calculated the ratio between corresponding polymerase-DNA dissociation constants. The dissociation constant in the absence of MarA is just K_R . The dissociation constant in the presence of MarA, K_R^+ , is determined by dissociation constants given in Table I using detailed balance (Fig. 4):

$$K_R^+ = \frac{K_X K_{AR}}{K_A}. \quad (7)$$

We calculated the ratio K_R^+/K_R and used the recruitment energy, e_r , to characterize the change in polymerase-DNA affinity upon MarA binding:

$$e_r = k_B T \ln \frac{K_X K_{AR}}{K_A K_R} = \Delta G_X + k_B T \ln K_{AR} - \Delta G_A - \Delta G_R. \quad (8)$$

From the definition of ΔG_X (Model), $\Delta G_X + k_B T \ln K_{AR}$ is equal to the free energy of the MarA-polymerase-DNA complex in the presence of 1 M free MarA and 1 M free polymerase. Therefore, from the definitions of ΔG_A and ΔG_R (Model) the recruitment energy e_r is equal to the free energy of interaction between MarA and polymerase on the DNA in the presence of 1 M each free MarA and free polymerase. A value $e_r = 0$ indicates no interaction between MarA and polymerase; a value $e_r < 0$ indicates that MarA attracts polymerase to the promoter; and a value $e_r > 0$ indicates that MarA repels polymerase from the promoter. Whereas the range of acceleration energies is determined by linear regression using the data, the recruitment energies are purely determined by the parameter values. For the parameter ranges in Table I, e_r assumes either positive or negative values (Fig. 3, right panels).

For *marRAB* and *soda*, the models with the lowest χ^2 have $e_r < 0$ (Fig. 3a, 3b, right panels; Table II). Activation in these models therefore involves attraction of polymerase to the promoter by

MarA. To determine the consequences of this attraction for polymerase binding to DNA, we compared the total occupancy of polymerase at the promoter,

$$P_{RX} = P_R + P_X, \quad (9)$$

in the presence (p_{RX}^+) vs. the absence (p_{RX}^-) of MarA. For both *marRAB* and *sodA*, the lowest- χ^2 models showed both a basal occupancy p_{RX}^- and ratio p_{RX}^+ / p_{RX}^- equal to 1 (Fig. 5a, 5b; Table II). The effect of the attraction is therefore insignificant with respect to recruiting polymerase to these promoters.

MarA repels polymerase from the *micF* promoter. For *micF*, the models with the lowest χ^2 have $e_r > 0$ (Fig. 3c, right panel; Table II). Activation in this model therefore involves *repulsion* of polymerase from the promoter by MarA. Moreover, unlike the neutral effect of attraction for *marRAB* and *sodA*, analysis of p_{RX}^+ / p_{RX}^- and p_{RX}^- indicates that repulsion leads to a decrease in the occupancy of polymerase at *micF* in the presence (0.93) vs. the absence (1.0) of MarA (Fig. 5a, Table II).

Results are robust to parameter variation. To quantify the degree of uncertainty in estimated parameter values within the nominal range, we calculated asymmetric errors of parameter values with respect to the optimum (Table II). The squared errors for parameter x were calculated using the equation

$$\sigma_{+x}^2 = \frac{\sum_i (x_i - x_{\min})^2 \theta(x_i - x_{\min}) e^{-x_i^2}}{\sum_i \theta(x_i - x_{\min}) e^{-x_i^2}}$$

$$\sigma_{-x}^2 = \frac{\sum_i (x_i - x_{\min})^2 \theta(x_{\min} - x_i) e^{-x_i^2}}{\sum_i \theta(x_{\min} - x_i) e^{-x_i^2}} \quad (9)$$

The likelihood function $e^{-\chi^2}$ in this analysis is arbitrary but is a standard choice (***)ref). The values of a_R , e_a , p_{RX}^- , and p_{RX}^+/p_{RX}^- in Table II are well-constrained by the data given the nominal ranges in parameter values (Table I). The value of e_r is less well-constrained, but the sign is robust to parameter variations. The absolute parameter values of K_R and K_X are very poorly constrained (not shown), but their ratio is well-constrained (and is related to e_r).

We also examined the sensitivity of the results to wider parameter variation (Parameter values, results not shown). Decreasing $[R]_T$ to 1,000 or 300 copies per cell led to significant increases in χ^2 , as did decreasing K_{AR} to 0.3 μM . With these exceptions, wider variation yielded models with minimum values of χ^2 comparable to those in Table II (values for *sodA* were as low as 2.16 for models with $K_{AR} = 100 \mu\text{M}$). The value of a_R was extremely robust to parameter variations (less than 1% change); in addition, p_{RX}^- remained close to 1 for models with low χ^2 over a wide range of parameter values. Values of other parameters varied more among low- χ^2 models; however, the qualitative mechanisms of acceleration and attraction (*marRAB*, *sodA*) or repulsion (*micF*) were robust to parameter variations.

Further validation of the model using CRP activation data. To further validate our promoter activity model, we used it to analyze published data on transcriptional activation of the *lac* operon by cAMP-CRP (4). The cAMP-CRP-dependent relative promoter activity was represented using the expression $y = 1 + 49x/(x + 5)$, where x is the concentration of the active CRP dimer in nM; this expression is consistent with the data published in Ref. (4). Consistent with expectations (3), we found that recruitment could be important for CRP activation of *lac* (Supplementary Fig. S2). Recruitment was significant when the dissociation constant between

polymerase and the promoter, K_R , was sufficiently large (K_R in excess of $\sim 100 \mu\text{M}$), and the recruitment effect increased with increasing K_R . By contrast, we were unable to find any good models for which recruitment is a significant factor in MarA activation of *mar*, *micF*, or *soda*, even for large values of K_R ; however, our results do not rule out this possibility.

Discussion and Conclusions

The present model of transcriptional regulation is consistent with available data on MarA-dependent promoter activity (13). The model therefore rationalizes the lack of correlation between measured MarA-DNA dissociation constants and level of MarA required for half-maximal promoter activation. In this regard, a critical feature of our model is explicit consideration of polymerase interactions with MarA both in the absence and in the presence of the promoter: Eq. (1) clearly emphasizes the importance of K_X , the dissociation constant between DNA and the MarA-polymerase complex, in determining the activation profile.

We expect interactions with polymerase to be similarly important for other activators, such as CRP, which also binds to polymerase away from the promoter (19). However, we expect interactions with polymerase to be less important when a repressor decreases expression by interfering with polymerase binding at the promoter. Such interference corresponds to very large values of K_X in our model, which increases the importance of K_A in determining the promoter activity profile. The correlation between a repressor's dissociation constant for binding to a recognition sequence and the level of repressor required for half-maximal repression is therefore expected to be high.

The model predicts that recruitment is not a significant factor in MarA activation of the *marRAB* and *soda*, and *micF* promoters. For all of these promoters, the model predicts that polymerase is

bound with near unit occupancy in the absence of MarA, and that activation occurs through an increase in polymerase activity when MarA is bound. It is important to note that our model was developed using data from *mar-rob-* strains (13), in which the repressor MarR is absent. In wild-type *E. coli*, we do expect polymerase to be bound at the *sodA* and *micF* promoters in the absence of inducers. However, in wild-type *E. coli*, MarR not only blocks polymerase binding but also blocks MarA binding at *marRAB* (20). We therefore do not expect polymerase to bind at the *marRAB* promoter in the absence of inducers that relieve MarR repression. These predictions are consistent with a genome-wide study of polymerase interactions with the *E. coli* chromosome (21), in which polymerase was detected at the *sodA* promoter but not the *marRAB* promoter (the study was inconclusive with respect to interactions at the *micF* promoter, which controls expression of an antisense mRNA transcript). The presence of polymerase at *sodA* in uninduced cells clearly represents an exception to the regulated recruitment model of transcriptional activation at σ^{70} promoters (1, 3), in which activation occurs solely through increasing the occupancy of polymerase at the promoter.

Because our model allows the values of a_X and a_R to differ, it is slightly more complex than the regulated recruitment model of transcriptional activation. This additional complexity is well-motivated when activator interacts with α -CTD of polymerase, as is the case for MarA. In the absence of activator, polymerase needs to disengage from sigma to escape the promoter; however, in the presence of activator, polymerase must sever its interactions with both sigma and activator. Because of this effect, tight interactions between activator and polymerase are expected to retard promoter escape and decrease the value of a_X compared to a_R . Our results support this expectation: e_a and e_r values in Table II (and for wider parameter ranges) are anti-correlated, indicating that stronger recruitment is associated with lower ratios a_X/a_R .

An unexpected result of our study is that activation of *micF* might involve repulsion of polymerase from the promoter by MarA. In light of the discussion above, it is possible that polymerase normally sits at the *micF* promoter, and that binding of activator accelerates the events up to and including promoter escape and message elongation, which effectively decreases the promoter affinity of polymerase. The possibility of this mechanism follows immediately from differentiating Eq. (4) with respect to $[A]_T$, which yields

$$a' = a_R p'_R + a_X p'_X. \quad (10)$$

Eq. (10) indicates that, for negative p'_R , positive p'_X , and negative $(p'_R + p'_X)$, a' can be positive for $a_X > -a_R p'_R / p'_X$. As this condition can only hold for $a_X > a_R$, repulsion decreases latency in transcription compared to regulated recruitment, which calls for $a_X = a_R$. In addition, whereas recruitment involves a decrease in the polymerase off rate in the presence of activator, repulsion involves an increase in the polymerase off rate; repulsion can therefore decrease latency in deactivation of promoters. Such decreases in latency might confer a competitive advantage to *E. coli* in an ecological context (22), increasing the significance of repulsion in transcriptional activation.

Acknowledgement. Supported by funding from the Department of Energy and the National Institutes of Health. We are grateful to Jelena Stajic, David Markowitz, and Luis Bettencourt for assistance in model development.

Figures and Tables

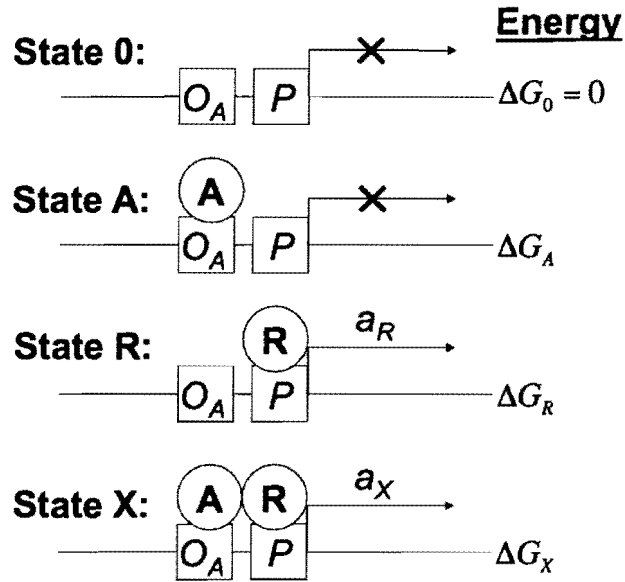
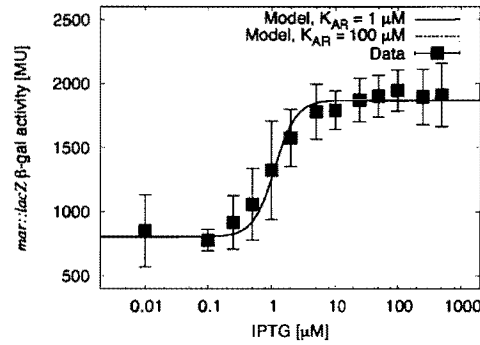
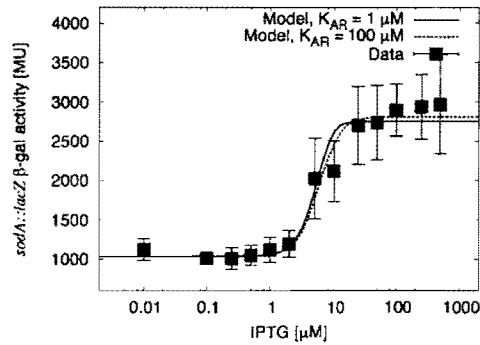


Figure 1. Promoter states and corresponding standard free energies.

a)



b)



c)

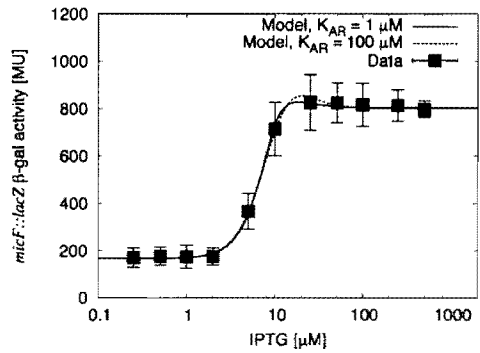


Figure 2: Fit of the best models of a) *marRAB* activation; b) *sodA* activation; and c) *micF* activation using either $K_{AR} = 1 \mu\text{M}$ (solid line) or $K_{AR} = 100 \mu\text{M}$ (dashed line). Corresponding χ^2 and parameter values are given in Table II.

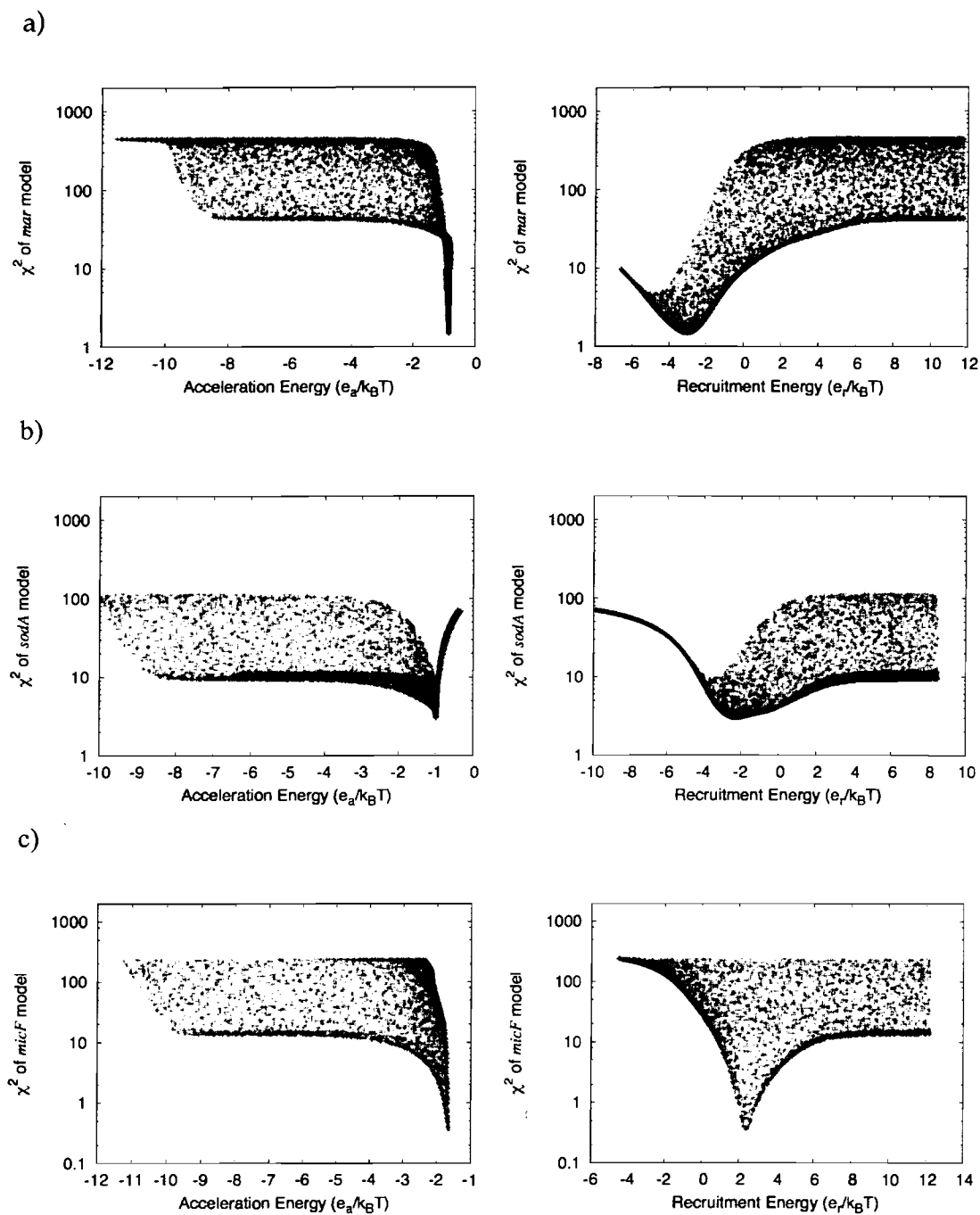


Figure 3. Dependence of χ^2 of a) *marRAB*, b) *sodaA*, and c) *micF* models on the acceleration energy (left panels) or attraction energy (right panels). Parameter values were sampled using the nominal values in Table I.

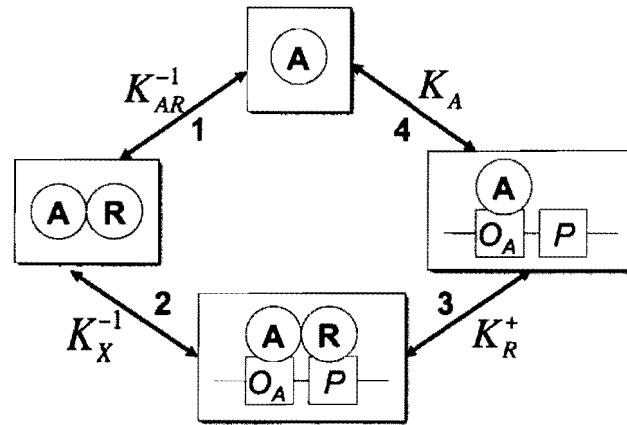
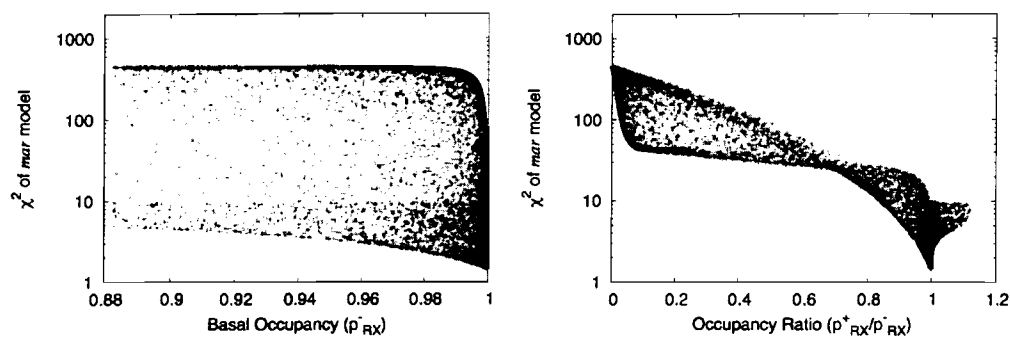
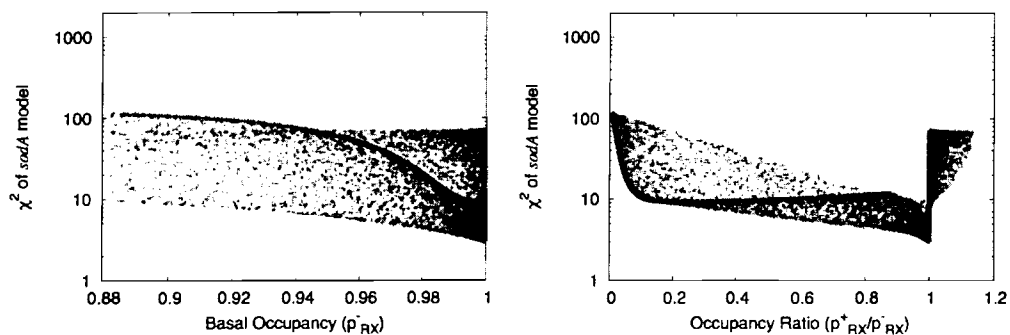


Figure 4. Determination of the polymerase-promoter dissociation constant in the presence of MarA (K_R^+). The above cycle, followed in a counterclockwise sense from the top, includes: (1) association of MarA and polymerase; (2) association of MarA-polymerase with the promoter; (3) dissociation of polymerase from the promoter when MarA is bound (the process of interest); and (4) dissociation of MarA from the promoter. Using detailed balance, the product of the equilibrium constants for (1)–(4) is equal to 1, yielding $K_R^+ = K_X K_{AR} / K_A$ (Eq. (7)).

a)



b)



c)

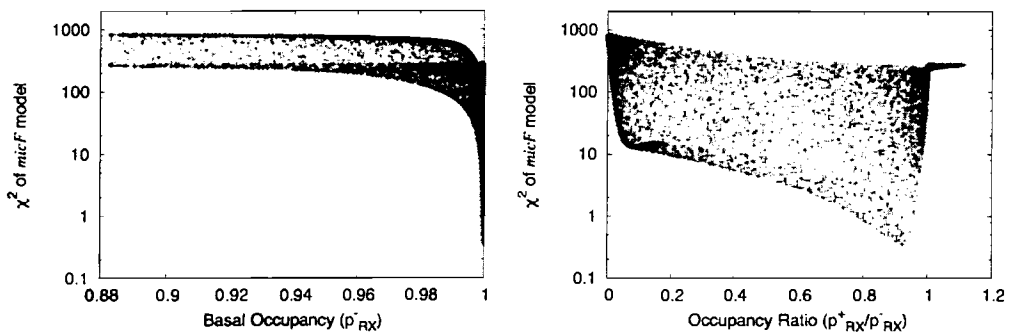


Figure 5. Dependence of χ^2 of a) *mar*, b) *sodA*, and c) *micF* models on the basal occupancy (left panel) or occupancy ratio (right panel). Parameter values were sampled using the nominal values in Table I. For the best models of all promoters, polymerase is bound at the promoter in the absence of activator. For the best models of *mar* and *sodA*, the occupancy essentially remains unchanged in the presence of activator. For the best model of *micF*, the occupancy *decreases* in the presence of activator.

Table I. Parameter values used to model activation of *marRAB*, *sodA*, and *micF* promoters by MarA.

Parameter	<i>marRAB</i>	<i>sodA</i>	<i>micF</i>
K_{AR} [μM]	1 ^a or 100 ^b	1 ^a or 100 ^b	1 ^a or 100 ^b
K_A [nM]	75	2,000	50
K_R [nM]	(1-1,000)	(1-1,000)	(1-1,000)
K_X [nM]	(0.01-100) K_R	(0.01-100) K_R	(0.01-100) K_R
$[R]_T$ [Molecules cell ⁻¹]	3,000	3,000	3,000
α_R [MU]	Eq. (4) regression	Eq. (4) regression	Eq. (4) regression
α_X [MU]	Eq. (4) regression	Eq. (4) regression	Eq. (4) regression

^a Nominal parameter value used to create Figs. 2-4.

^b Secondary parameter value used to create Fig. 2.

Table II. Properties of models with the lowest value of χ^2 . Asymmetric errors calculated using all samples are indicated in parentheses. Parameter values were sampled using nominal values and ranges in Table I. Values of x are listed with asymmetric errors σ_{+x} and σ_{-x} as $x(+\sigma_{+x})(-\sigma_{-x})$ (errors are defined in Eq. (9)).

	<i>marRAB</i>	<i>sodA</i>	<i>micF</i>
Minimum χ^2	1.472	3.023	0.353
a_R [MU]	807(+15)(-20)	1,039(+12)(-9)	168(+6)(-5)
$e_a/k_B T$	-0.84(+0.01)(-0.02)	-0.98(+0.01)(-0.3)	-1.652(+0.006)(-0.1)
$e_r/k_B T$	-3.0(+0.7)(-1.0)	-2.2(+1.6)(-0.7)	+2.4(+0.7)(-0.3)
p_{RX}^-	1.000(+2×10 ⁻⁷)(-0.012)	1.000(+2×10 ⁻⁵)(-0.006)	1.000(+2×10 ⁻⁵)(-2×10 ⁻⁴)
p_{RX}^+ / p_{RX}^-	1.000(+0.009)(-0.01)	0.9993(+6×10 ⁻⁴)(-0.08)	0.93(+0.2)(-0.1)

References

1. Ptashne M (2003) Regulated recruitment and cooperativity in the design of biological regulatory systems. *Philos Transact A Math Phys Eng Sci* 361:1223-1234.
2. Ptashne M & Gann A (1997) Transcriptional activation by recruitment. *Nature* 386:569-577.
3. Ptashne M & Gann A (2002) *Genes & Signals* (Cold Spring Harbor Press, Cold Spring Harbor, NY).
4. Bintu L, *et al.* (2005) Transcriptional regulation by the numbers: applications. *Curr Opin Genet Dev* 15:125-135.
5. Bintu L, *et al.* (2005) Transcriptional regulation by the numbers: models. *Curr Opin Genet Dev* 15:116-124.
6. Summers AO (1992) Untwist and shout: a heavy metal-responsive transcriptional regulator. *J Bacteriol* 174:3097-3101.
7. Hidalgo E & Dimple B (1994) An iron-sulfur center essential for transcriptional activation by the redox-sensing SoxR protein. *EMBO J* 13:138-146.
8. Kolb A, Busby S, Buc H, Garges S, & Adhya S (1993) Transcriptional regulation by cAMP and its receptor protein. *Annu Rev Biochem* 62:749-795.
9. Menendez M, Kolb A, & Buc H (1987) A new target for CRP action at the *malT* promoter. *EMBO J* 6:4227-4234.
10. Martin RG, Gillette WK, Rhee S, & Rosner JL (1999) Structural requirements for *mar* box function in transcriptional activation of *mar/sox/rob* regulon promoters in *Escherichia coli*: sequence, orientation and spatial relationship to the core promoter. *Mol Microbiol* 34:431-441.
11. Wood TI, *et al.* (1999) Interdependence of the position and orientation of SoxS binding

- sites in the transcriptional activation of the class I subset of *Escherichia coli* superoxide-inducible promoters. *Mol Microbiol* 34:414-430.
12. White DG, Alekshun MN, & McDermott PF (2005) *Frontiers in Antimicrobial Resistance* (ASM Press, Washington, DC).
 13. Martin RG, Bartlett ES, Rosner JL, & Wall ME (2008) Activation of the *Escherichia coli* marA/soxS/rob regulon in response to transcriptional activator concentration. *J Mol Biol* 380:278-284.
 14. Ackers GK, Johnson AD, & Shea MA (1982) Quantitative model for gene regulation by lambda phage repressor. *Proc Natl Acad Sci U S A* 79:1129-1133.
 15. Martin RG, Gillette WK, Martin NI, & Rosner JL (2002) Complex formation between activator and RNA polymerase as the basis for transcriptional activation by MarA and SoxS in *Escherichia coli*. *Mol Microbiol* 43:355-370.
 16. Marr MT & Roberts JW (1997) Promoter recognition as measured by binding of polymerase to nontemplate strand oligonucleotide. *Science* 276:1258-1260.
 17. Ishihama A (2000) Functional modulation of *Escherichia coli* RNA polymerase. *Annu Rev Microbiol* 54:499-518.
 18. Meuller-Hill B (1996) *The lac operon* (Walter de Gruyter, Berlin).
 19. Heyduk T, *et al.* (1993) CAP interacts with RNA polymerase in solution in the absence of promoter DNA. *Nature* 364:548-549.
 20. Martin RG, Jair KW, Wolf RE, Jr., & Rosner JL (1996) Autoactivation of the marRAB multiple antibiotic resistance operon by the MarA transcriptional activator in *Escherichia coli*. *J Bacteriol* 178:2216-2223.
 21. Grainger DC, Hurd D, Harrison M, Holdstock J, & Busby SJ (2005) Studies of the distribution of *Escherichia coli* cAMP-receptor protein and RNA polymerase along the E.

coli chromosome. *Proc Natl Acad Sci U S A* 102:17693-17698.

22. Savageau MA (1974) Comparison of classical and autogenous systems of regulation in inducible operons. *Nature* 252:546-549.